Original Research

T2-Weighted and Diffusion-Weighted MRI for Discriminating Benign From Malignant Focal Liver Lesions: Diagnostic Abilities of Single Versus Combined Interpretations

Hiroki Haradome, MD, PhD,[1,2*] Luigi Grazioli, MD, PhD,[1] Mario Morone, MD,[1] Sebastiana Gambarini, MD,[1] Thomas C. Kwee, MD,[3] Taro Takahara, MD, PhD,[3] and Stefano Colagrande, MD, PhD[4]

Purpose: To compare the diagnostic accuracies of diffusion-weighted imaging (DWI), T2-weighted imaging (T2WI), and the combination of both sequences in discriminating benign from malignant focal liver lesions (FLLs).

Materials and Methods: In all, 166 patients with 269 FLLs (153 benign and 116 malignant) were retrospectively evaluated. Two abdominal readers visually assessed the DWI, T2WI, and the combined (DWI+T2WI) image sets in an independent and blinded manner. The diagnostic abilities of each image set in discriminating the benign from the malignant FLLs set were compared using a binary logistic regression model. Pathologic results, consensus reading, and follow-up imaging were used as the reference standard.

Results: The overall characterization accuracy in all lesions of the combined set (80.3%) was significantly higher than those of the T2WI set (68.8%) and DWI set (73.2%) (combined vs. T2WI, $P < 0.001$; combined vs. DWI, $P = 0.001$), while there was no significant difference between the T2WI and DWI sets ($P = 0.058$). All image sets were more accurate in the characterization of malignant FLLs than of benign FLLs ($P < 0.001$).

Conclusion: T2WI and DWI are complementary in discriminating benign from malignant FLLs; their combination improves diagnostic confidence.

Key Words: diffusion-weighted imaging; T2-weighted imaging; focal liver lesions
J. Magn. Reson. Imaging 2012; 000:000–000.

MAGNETIC RESONANCE IMAGING (MRI) yields excellent tissue contrast through a wide range of pulse sequences and can visualize the internal structures and several functional processes in the body. Beyond controversy, dynamic enhanced MRI with several contrast agents has a major role in the detection and characterization of focal liver lesions (FLLs). However, unenhanced MR sequences such as T2-weighted imaging (T2WI) and diffusion-weighted imaging (DWI) could provide additional important information for the differential diagnosis of FLLs and they cannot be omitted from a state-of-the-art MR liver protocol. Furthermore, in those patients with contraindications to contrast agents, the unenhanced MR sequences become crucial in the characterization of FLLs. Classically, T2WI is considered a useful sequence for discriminating benign cystic lesions (eg, simple cyst, hemangioma, etc) from malignant solid lesion (eg, metastasis, hepatocellular carcinoma [HCC], etc) on the basis of the degree of the signal intensity of the lesion, but its utility in the differentiation between solid benign and malignant lesions may be limited. DWI is another useful sequence, which provides tissue contrast based on the diffusion properties of water molecules in tissue, without using any contrast agents. Based on a series of recent advances in MRI, including high-performance gradient systems, single-shot echo-planar imaging (EPI), and parallel acquisition techniques (eg, sensitivity encoding: SENSE), abdominal DWI is increasingly being applied for lesion detection and characterization (1–12), monitoring and predicting treatment response (13–16), and assessment of chronic liver disease (17,18). DWI not only is able to provide a high lesion-to-background contrast compared to other unenhanced MR sequences (7,9,11,12), it also provides (quantitative) physiological information by means of apparent diffusion coefficient (ADC) measurements. ADCs are, among others, thought to reflect tissue cellularity and cell membrane integrity, and may aid in lesion characterization. In the past decade, several researchers indicated the

[1]Department of Radiology, University of Brescia, Spedali Civili di Brescia, Brescia, Italy.
[2]Department of Radiology, Kyorin University School of Medicine, Tokyo, Japan.
[3]Department of Radiology, University Medical Center Utrecht, Utrecht, De Uithof, Nederland.
[4]Department of Radiology, University of Florence, Azienda Ospedaliero-Universitaria Careggi, Firenze, Italy.
*Address reprint requests to: H.H., Piazzale Spedali Civili 1, 25123, Brescia (BS), Italy. E-mail: karate.b@gmail.com
Received February 11, 2011; Accepted December 7, 2011.
DOI 10.1002/jmri.23573
View this article online at wileyonlinelibrary.com.

utility of abdominal DWI in the differentiation of FLLs, although overlaps in ADCs are observed between some benign and malignant tumors (1–11). The relatively low spatial resolution and the signal loss in the left hepatic lobe due to cardiac pulsation are some of the limitations of DWI. Therefore, DWI has not yet replaced T2WI in routine protocols because it simultaneously has several intrinsic advantages and realistic limitations. Until now, there have only been a few comparative investigations between T2WI and DWI in the characterization of FLLs (11,19), and those studies (11,19) did not include a large number and wide spectrum of FLLs, in particular solid benign tumors (eg, focal nodular hyperplasia [FNH] and adenoma). Furthermore, to our knowledge, there is no published study that investigated the diagnostic ability of the combined interpretation of both sequences compared to each sequence alone.

The purpose of this study was therefore to compare the diagnostic accuracies of DWI alone, T2WI alone, and a combined interpretation of the two sequences for discriminating benign from malignant FLLs, in a large number of patients with a wide spectrum of FLLs.

MATERIALS AND METHODS

Our Institutional Review Board approved this retrospective study. Written informed consent from patients was waived. All data and information derived from and pertaining to the study were under the exclusive control of the investigating radiologists.

Patients

We retrospectively reviewed our hospital reporting database of MR examinations (including DWI) for patients suspected of having FLLs for the period between June 2008 and February 2010. A total of 348 patients who were suspected of having FLLs were identified. Among these patients, 182 patients were excluded because of 1) having no FLL ($n = 92$); 2) only having FLLs with a maximum diameter of less than 5 mm (as measured on dynamic contrast-enhanced images, including hepatobiliary phase images, with conventional gadolinium chelates or hepatocyte-specific agents [eg, Gd-BOPTA or Gd-EOB-DTPA]) in which unfavorable partial volume effects frequently occur ($n = 31$); 3) clinical and imaging follow-up of less than 6 months ($n = 36$); 4) regional therapy (transarterial chemoembolization, radiofrequency ablation, or percutaneous ethanol injection) or systemic chemotherapy before MRI, which could affect signal of the lesions at DWI ($n = 23$).

Hence, a total of 166 patients (76 men, 90 women; mean age [± standard deviation], 56.0 ± 16.1 years; age range, 12–87 years) with 269 FLLs (lesions with a maximum diameter of less than 5 mm were excluded) were enrolled in this study (Table 1).

There were 42 patients with chronic liver disease, including 10 with chronic hepatitis and 31 with liver cirrhosis related to viral hepatitis B ($n = 15$), viral hepatitis C ($n = 20$), viral hepatitis B and C ($n = 1$), or alcohol abuse ($n = 6$). There were six patients with steatosis and 119 patients with a normal background liver parenchyma.

Table 1
Clinical Information of the 166 Patients and Characteristics of 269 Focal Liver Lesions

Age range (mean age)	12-87 years (56.0 years)
Sex (M/F)	76/90
Diagnosis of the lesions ($n = 269$)	
Benign ($n = 153$)	51 hemangioma
	54 FNH
	17 adenoma
	28 cyst
	2 pseudotumor
	1 abscess
Malignant ($n = 116$)	55 HCC
	34 metastasis
	22 CCC
	5 lymphoma
Location of the lesions	100 right lobe 169 left lobe
Background liver	10 chronic hepatitis
	31 liver cirrhosis
	6 steatosis
	119 normal liver
Primary site of metastatic patients ($n = 18$)	10 colon
	3 breast
	2 kidney
	1 stomach
	1 pancreas
	1 gastrointestinal tumor

FNH: focal nodular hyperplasia; HCC: hepatocellular carcinoma; CCC: cholangiocellular carcinoma; LC: liver cirrhosis.

The metastases in the 18 patients with metastatic liver disease originated from colon ($n = 10$), breast ($n = 3$), kidney ($n = 2$), stomach ($n = 1$), and pancreas cancer ($n = 1$), and a gastrointestinal tumor ($n = 1$). Multiple lesions (range, 2–5 lesions) were noted in 45 of the 166 patients and different histologic types of lesions (eg, HCC and hemangioma) coexisted in 23 patients.

FLLs and Standard of Reference

The final diagnosis of each FLL was based on pathologic results, consensus reading by two qualified abdominal radiologists with more than 10 years of experience using precontrast and dynamic contrast-enhanced MR images, clinical information, and/or follow-up imaging evaluations. Finally, 269 FLLs (153 benign and 116 malignant lesions) with an average diameter of 30.4 ± 22.0 mm (range, 6–150 mm) were confirmed through this process. The 153 benign lesions consisted of 51 hemangiomas, 28 cysts, 54 FNHs, 17 adenomas, two pseudotumors, and one abscess, while the 116 malignant lesions consisted of 34 metastases, 55 HCCs, 22 cholangiocarcinomas (CCCs), and five lymphomas (Table 1). In all, 100 of 269 FLLs were located in the left lobe (S1–4) and the remaining 169 were located in the right lobe (S5–8).

Among 153 benign lesions, 32 lesions were diagnosed histopathologically: all 17 adenomas (five by

resection and 12 by biopsy), 11 FNHs (all by biopsy), three hemangiomas (all by biopsy) and one abscess (by fluid drainage). In the remaining 119 lesions, except for the two pseudotumors (47 hemangiomas, 44 FNHs, and all 28 cysts), the diagnosis was established based on laboratory findings, established characteristic imaging criteria (20–23), and their stable appearance in size at follow-up imaging studies. The existence of two pseudotumors in one patient was confirmed based on a decrease in their size on serial follow-up imaging evaluations. In 42.6% (23/54) of FNHs a central scar was identified within the mass on dynamic contrast-enhanced MR images.

Among 116 malignant lesions, 76 lesions were diagnosed histopathologically: 34 HCCs (11 by resection and 23 by biopsy), 19 CCCs (seven by resection and 12 by biopsy), 18 metastases (all by biopsy), and all five lymphomas (two by resection and three by biopsy). The 21 HCCs in 14 cirrhotic patients and the three CCCs in two patients (who did not have any other extrahepatic malignant lesions, which may have caused hepatic metastasis) were diagnosed by characteristic imaging findings (23–27), including the American Association for the Study of Liver Disease (AASLD) criteria for HCC (28) and elevated tumor markers (eg, α-fetoprotein and plasma prothrombin in vitamin K absence for HCC, and carbohydrate antigen 19-9 for CCC). The diagnosis of 16 metastases was based on follow-up imaging studies (range, 94–158 days), which showed size progression.

MRI

MRI was performed using a 1.5-T scanner with an 18-channel system (Avanto, Siemens Medical Systems, Erlangen, Germany) equipped with high-performance gradients (maximum gradient strength of 45 mT/m; peak slew rate of 200 mT/m/ms) and a 12-element (dorsoabdominal two six-element) surface phased-array coil in all patients.

Before administration of contrast agent, a breath-hold dual-echo T1-weighted gradient-dual echo sequence, a navigator-triggered T2-weighted turbo spin-echo (TSE) sequence with and without fat-suppression, and a navigator-triggered DWI were obtained in transverse directions as precontrast images. After scanning these precontrast images, fat-saturated dynamic contrast-enhanced 3D gradient-echo sequences with volumetric interpolated breath-hold examination image (VIBE; Siemens) were performed.

Integrated parallel imaging techniques (iPAT) using generalized autocalibrating partially parallel acquisition (GRAPPA) with an acceleration factor of two were applied to all sequences to shorten the echo train length (ETL) in order to improve image quality and reduce acquisition time.

For respiratory triggering, we used the prospective acquisition correction (PACE; Siemens Medical Solutions), which measures the temporal position of the diaphragm during free breathing.

The PACE technique and a single-shot spin-echo EPI sequence, accommodating four motion probing gradients, were applied for navigator-trigged DWI. Navigator-trigged DWI was performed with the following parameters: TR/TE, 2000/71 msec; echo train length, 77; bandwidth, 1628 Hx/pixel; field of view (FOV), 320–450 mm; spectral attenuated inversion recovery (SPAIR); matrix size, 77 × 192; number of signal averages, 3; section thickness/gap, 6/1 mm; 28–38 sections; acquisition time, 4–5 minutes. Tridirectional motion probing gradients with different b-values (50, 400, and 800 s/mm^2) were applied in one acquisition. The diffusion-weighted images with a low b-value (50 s/mm^2) served as a black blood image with high signal-to-noise ratio.

Respiratory-triggered T2-weighted TSE sequences with and without fat-suppression were obtained with the following parameters: TR/TE, 2120/79 msec; ETL, 14; flip angle, 150°, section thickness/gap, 6/1 mm; 28–38 sections; FOV, 380–500 mm; matrix size, 81 × 320; number of signal averages, 1; acquisition time, 3–5 minutes.

Imaging Analysis

All MR images were independently interpreted by two abdominal radiologists who were blinded to all clinical information, including MRI reports, clinical history, pathologic findings, and other MR sequences (eg, dynamic contrast-enhanced MRI) using a local picture archiving and communication system monitor (iSite Radiology, Philips Healthcare, Best, Netherlands). The two readers evaluated three image datasets: 1) DWI alone; 2) T2WI (with and without fat-suppression) alone; and 3) the combination of both (DWI and T2WI), with a 1-month interval between the evaluation of different image sets. Before each reading session, the two readers were trained using some representative cases (which were not included in this analysis) in order to become familiar with the predefined imaging criteria for FLL characterization at DWI and T2WI.

Based on lesion morphology and degree and homogeneity of lesion signal on each image, the readers categorized all lesions as benign or malignant using the following three-point grading scale: 1 = benign; 2 = indeterminate; 3 = malignant, as some authors adopted in recent articles (11). For the evaluation of DWI, both the images obtained with three different b-values (50, 400, and 800 s/mm^2) and the ADC maps were assessed and the following criteria were used (2,3,6,11) (Fig. 1): a lesion was regarded as benign, if the lesion was hyperintense at DWI obtained with a b-value of 50 s/mm^2, showing signal intensity decrease with increasing b-values, and exhibited subjectively hyperintensity to the surrounding liver parenchyma on ADC maps. A lesion was regarded as malignant if the lesion was hyperintense at DWI obtained with a b-value of 50 s/mm^2 and the signal remained hyperintense at DWI obtained with a b-value of 800 s/mm^2, and exhibited hypointensity relative to the surrounding liver parenchyma on ADC maps. A lesion was regarded as indeterminate if the lesion did not fulfill either of these imaging criteria.

For the evaluation of T2-weighted images, the following criteria were used (29–31) (Fig. 1): a lesion was regarded as benign if the lesion showed a well-defined

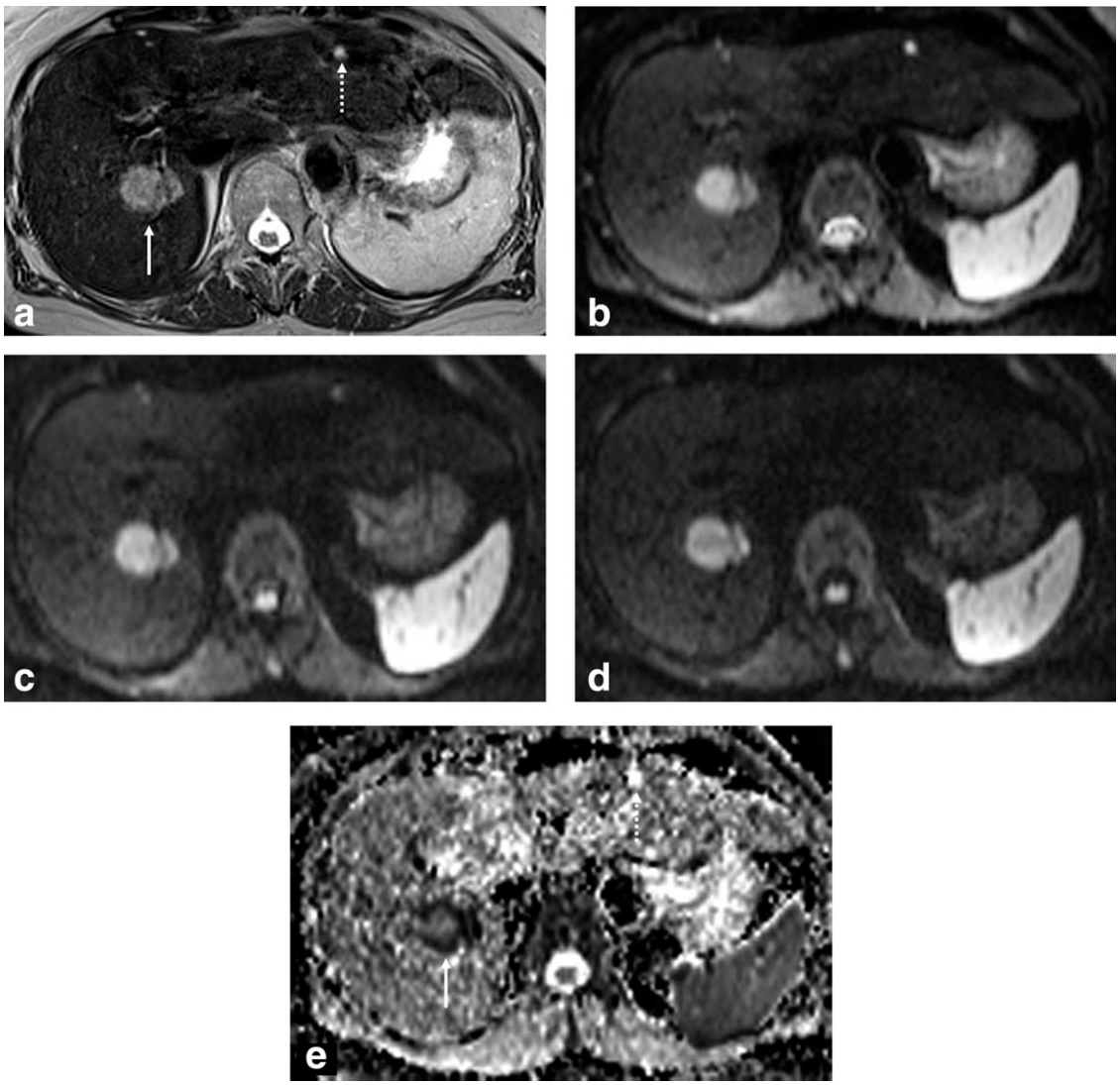

Figure 1. Metastasis from colon cancer and small cysts in a 67-year-old man. Transverse T2-weighted image (**b–d**). Transverse DWIs obtained with b-values of 50 (b), 400 (c), and 800 (d) s/mm^2, (**e**) ADC map. At T2WI (**a**), metastasis (solid arrow) in segment VI is moderately hyperintense and a small cyst (dotted arrow) in segment III shows marked hyperintensity relative to surrounding liver parenchyma. On navigator-triggered DWIs (b–d), the metastasis with restricted diffusion is moderately hyperintense at a b-value of 50 s/mm^2 and the signal is largely retained at a b-value of 800 s/mm^2, which is compatible with a malignant lesion. On the other hand, the small cyst containing free water is markedly hyperintense at a b-value of 50 s/mm^2 and the signal completely disappears at a b-value of 800 s/mm^2, which is a typical feature of a benign lesion. On the ADC map (e), the metastasis is hypointense (solid arrow), which corresponds to a low ADC (0.89×10^{-3}mm^2/s) and the small cyst shows distinct hyperintensity (dotted arrow) with a high ADC (2.97×10^{-3}mm^2/s) relative to the surrounding liver parenchyma.

margin and homogeneous marked hyperintensity relative to the surrounding liver parenchyma. A lesion was regarded as malignant if the lesion showed ill-defined margins and heterogeneous mild to moderate hyperintensity relative to the surrounding liver parenchyma. A lesion was regarded as indeterminate if the lesion did not fulfill either of these imaging criteria (eg, a lesion showing isointensity relative to the surrounding liver parenchyma). Based on these criteria, the readers classified all lesions into three categories (benign, indeterminate, and malignant) at DWI and T2WI separately. In the combined reading session, the reader classified all lesions using both criteria for DWI and T2WI at their discretion.

Statistical Analysis

The diagnostic efficacies of T2WI alone, DWI alone, and the combination of both sequences for visual discrimination between benign and malignant liver lesions were evaluated. A lesion characterization identical to the definitive diagnosis (benign or malignant) was defined as a correct diagnosis, whereas a characterization not identical to the definitive diagnosis or characterization as indeterminate was defined as an incorrect diagnosis. A statistical analysis was done by using a binary logistic regression model in which the diagnostic accuracy was included as a dependent variable.

Table 2
Correctly Characterized FLLs With Each Sequence in All, Benign, Malignant Lesions

Sequence		All lesions ($n = 269$)	Benign lesions ($n = 153$)	Malignant lesions ($n = 116$)
DWI		73.2 (197/269)	64.7 (99/153)	84.5 (98/116)
T2WI		68.0 (183/269)	50.3 (77/153)	91.4 (106/116)
Combined		80.3 (216/269)	67.0 (102.5/153)	97.8 (113.5/116)
P value	DWI vs. T2WI	0.058	<0.001	0.011
	DWI vs. Combined	0.001	0.504	<0.001
	T2WI vs. Combined	<0.001	<0.001	0.004

Data are averaged for two independent observers. Unless otherwise indicated, numbers are percentages, with raw data in parentheses.
DWI: diffusion-weighted imaging; T2WI: T2-weighted imaging; Combined: DWI+T2WI.

In consideration of a potential lesion correlation within the same patient, the analysis was performed using a generalized linear mixed model including patient and lesion as random effects and MR sequence (T2WI vs. DWI vs. T2WI+DWI), reader (reader 1 vs. reader 2), and definitive diagnosis (benign vs. malignant) as fixed effects. An interaction between readers and diagnostic imaging modalities was also included in the model.

Similar analyses were also performed in subgroups according to the definitive diagnosis (benign or malignant lesions). In these subgroup analyses the definitive diagnosis was excluded from the model. We evaluated the diagnostic capabilities using an adjusted odds ratio (OR) and a *P* value. A *P* value of less than 0.05 was considered significant. Reader agreement at T2WI and DWI was analyzed using the weighted κ statistic, defined as poor (<0.2), fair (>0.2 to ≤0.4), moderate (>0.4 to ≤0.6), good (>0.6 to ≤0.8), and excellent (>0.8 to ≤1) agreement. All analyses were performed using commercial statistical software (SAS, v. 9.0 and JMP, v. 8; SAS Institute Japan, Tokyo, Japan).

RESULTS

Visual Assessment

Correctly characterized FLLs using the different sequences (T2WI and DWI) and their combination in all, benign, and malignant lesions are shown in Table 2.

The overall characterization accuracies in all lesions with T2WI, DWI, and the combined (T2WI+DWI) sets were 68.0%, 73.2%, and 80.3%, respectively. There was a significant difference between T2WI and the combined set (adjusted OR, 8.457, $P < 0.001$) and between DWI and the combined sets (adjusted OR, 4.268, $P = 0.001$).

Meanwhile, no significant difference was observed in the characterization accuracy between the T2WI and DWI sets (adjusted OR, 1.984, $P = 0.058$).

All image sets were more accurate in the characterization of malignant FLLs than of benign FLLs (adjusted OR, 68.204, $P < 0.001$).

The correctly characterized FLLs using the different sequences (T2WI and DWI) and their combination by each reader in all, benign, and malignant lesions are shown in Table 3. The subgroup analysis in the benign lesions showed no significant interaction between readers on each MR sequence. In a comparison of all sequences in the benign lesions, the characterization accuracies with T2WI, DWI, and the combined sets were 50.3%, 64.7%, and 67.0%, respectively, showing a significant difference between DWI and T2WI sets and between the combined and T2WI sets (DWI vs. T2WI: adjusted OR, 34.679, $P < 0.001$; the combined vs. T2WI: adjusted OR, 48.285, $P < 0.001$). In the characterization accuracy of the benign lesions, no significant difference was observed between DWI and the combined sets (adjusted OR, 1.500, $P = 0.504$).

The subgroup analysis in the malignant lesions showed a significant effect of the readers on characterization accuracy. The characterization accuracy of reader 2 was significantly lower than that of reader 1 (adjusted OR, 0.200, $P = 0.045$). In a comparison of all sequences in the malignant lesions, the characterization accuracies with T2WI, DWI, and the combined sets were 91.4%, 84.5%, and 97.8%, respectively. There was a significant difference in characterization accuracy of the malignant lesions between T2WI and DWI sets, between T2WI and the combined sets, and between DWI and the combined sets (T2WI vs. DWI: adjusted OR, 0.401, $P = 0.011$. T2WI vs. the combined interpretation: adjusted OR, 5.800, $P = 0.004$. DWI vs. the combined: adjusted OR, 14.469, $P < 0.001$).

Table 3
Correctly Characterized FLLs With Each Sequence by the Two Readers in All, Benign, Malignant Lesions

	Sequence	All lesions ($n = 269$)	Benign lesions ($n = 153$)	Malignant lesions ($n = 116$)
Reader 1	DWI	73.6 (198/269)	64.1 (98/153)	86.2 (100/116)
	T2WI	69.5 (187/269)	50.3 (77/153)	94.8 (110/116)
	Combined	80.3 (216/269)	65.4 (100/153)	100.0 (116/116)
Reader 2	DWI	72.9 (196/269)	65.4 (100/153)	82.8 (96/116)
	T2WI	66.5 (179/269)	50.3 (77/153)	87.9 (102/116)
	Combined	80.3 (216/269)	68.6 (105/153)	95.7 (111/116)

Unless otherwise indicated, numbers are percentages, with raw data in parentheses.
DWI: diffusion-weighted imaging; T2WI: T2-weighted imaging; Combined: DWI+T2WI.

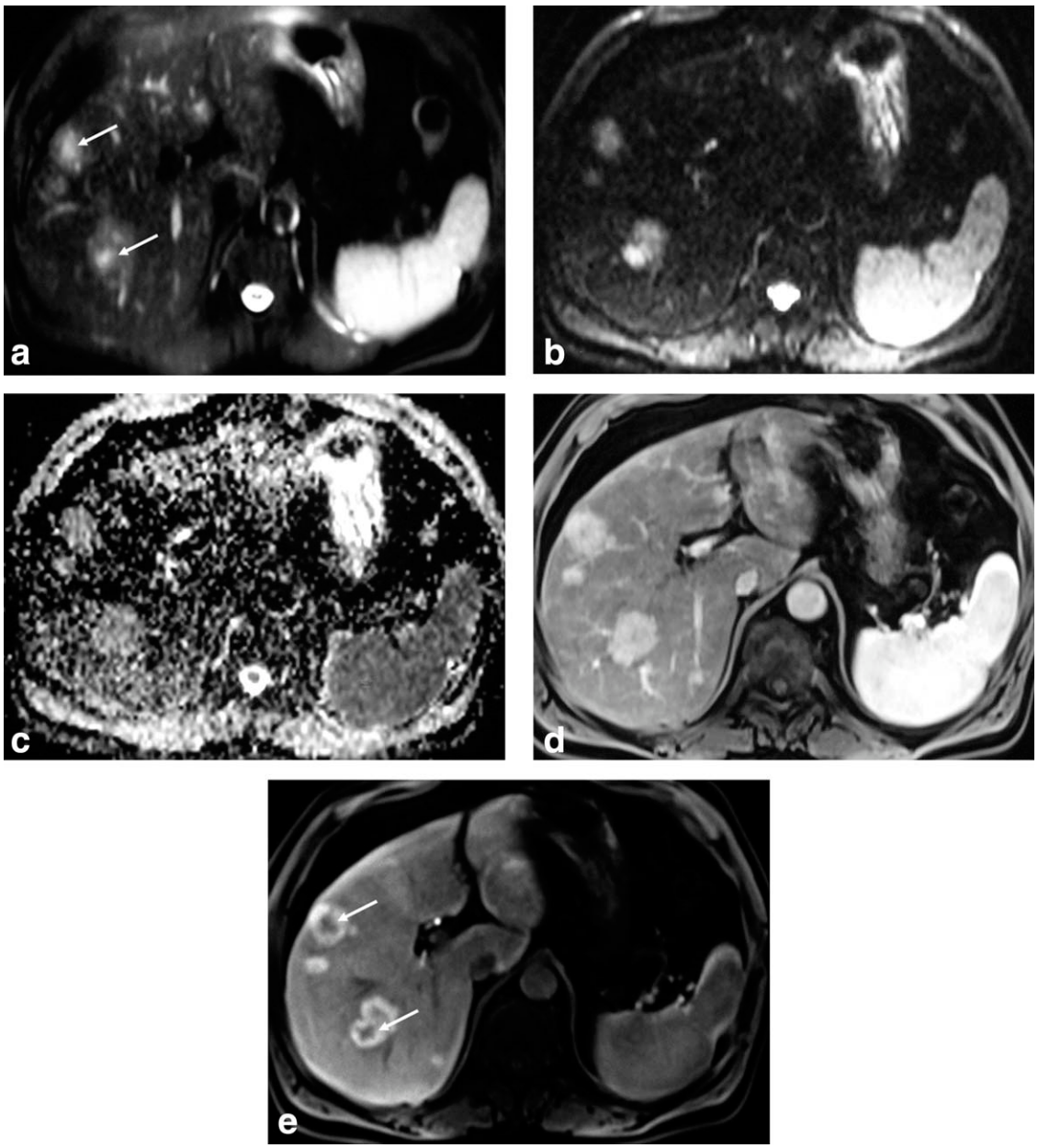

Figure 2. Multiple FNHs in a 63-year-old man. **a**: Transverse fat saturated T2-weighted image. **b**: Transverse DWIs obtained with a b-value of 50 s/mm^2, and (**c**) ADC map (**d**) dynamic contrast-enhanced MR images with Gd-EOB-DTPA in the arterial phase (**e**) and in the hepatobiliary phase. On fat-saturated T2-weighted images, three FNHs with moderately high signal are shown in segments VII–VIII. The margins of the three lesions are irregular and the central parts of the two larger lesions (arrows) show markedly high signal intensity on the T2-weighted images. The two FNHs were misjudged as malignant lesions (a score of 3) by both readers because they mimicked metastatic lesions with central necrosis. The three FNHs also display moderately high signal intensity at DWI obtained with a b-value of 50 s/mm^2. On the corresponding ADC map, the three FNHs demonstrate clear hyperintensity with relatively high ADCs (1.48×10^{-3}mm^2/s) compared to surrounding liver parenchyma, and the lesions were correctly judged as benign (a score of 1) by both readers. The three FNHs demonstrate intense arterial enhancement and remain hyperintense in the hepatobiliary phase, which are typical features of FNH. The central hypointense areas (arrows) within the masses are shown on the hepatobiliary phase image, which corresponds to central vascular scars.

Reader agreement for the visual discrimination between benign and malignant lesions using T2WI alone, DWI alone, and the combined interpretation was excellent, given the κ values of 0.921 (95% confidence interval [CI]: 0.881–0.961), 0.923 (95% CI: 0.882–0.962), 0.932 (95% CI: 0.892–0.964), respectively.

Misclassified Lesions

The 18 benign lesions misjudged as malignant by both readers at T2WI included eight FNHs (14.8%, 8/54) (Fig. 2), seven adenomas (41.2%, 7/17), one hemangioma (1.96%, 1/51), one (100%, 1/1) abscess, and one pseudotumor (50%, 1/2).

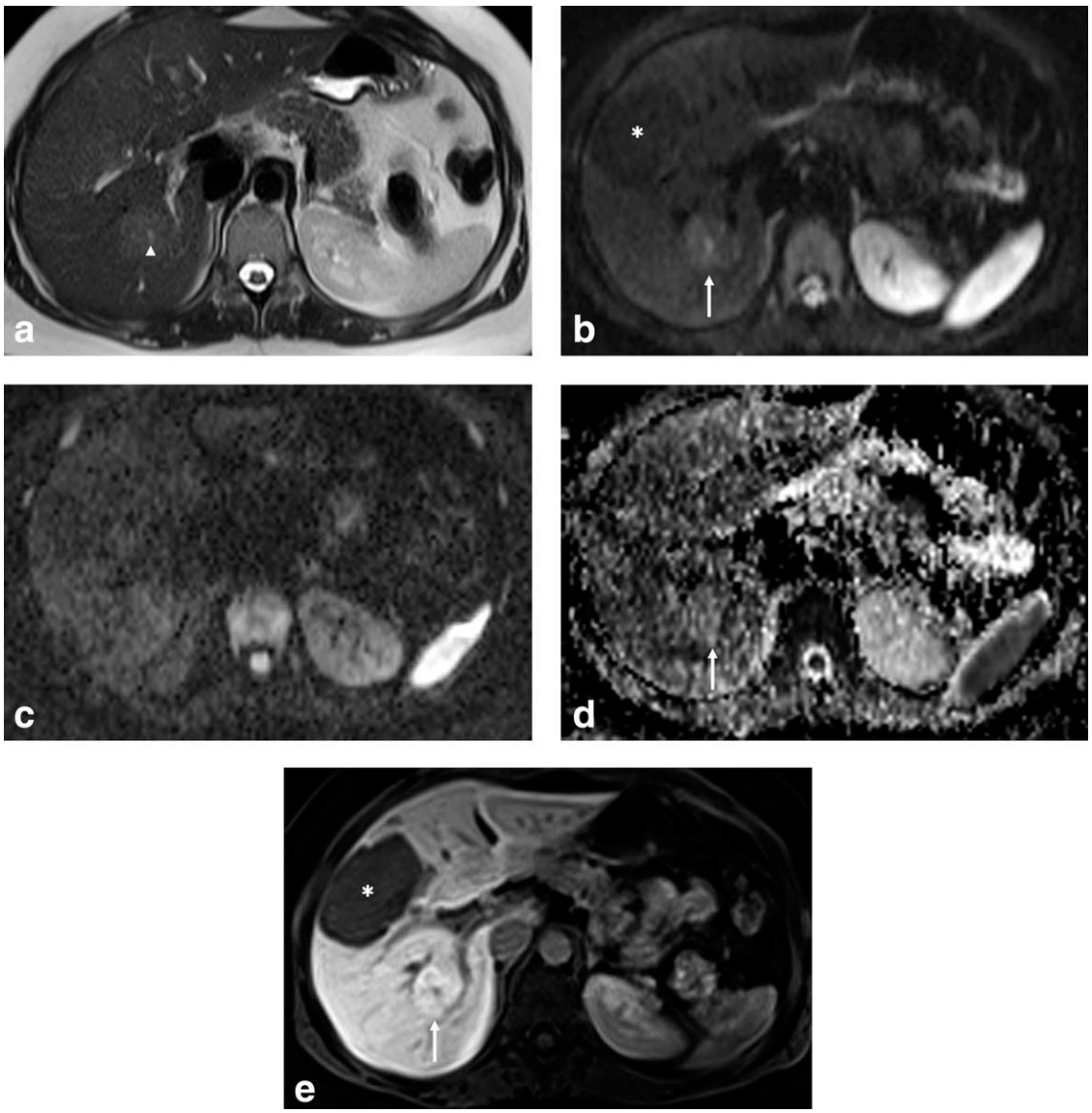

Figure 3. Adenoma and FNH in a 31-year-old woman. **a**: Transverse T2-weighted image. **b,c**: Transverse DWIs obtained with b-values of 50 (b) s/mm^2 and 800 (c) s/mm^2, (**d**) ADC map, and (**e**) hepatobiliary phase MR image with Gd-EOB-DTPA. At T2WI, the adenoma is isointense and the FNH with tiny scar (arrowhead) is mildly hyperintense relative to the surrounding liver parenchyma. Both lesions were judged as indeterminate (a score of 2 was assigned) by both readers. On DWIs the adenoma (asterisk) demonstrates slightly hypointensity relative to the surrounding liver parenchyma, while FNH (arrow) displays mild hyperintensity at a b-value of 50 s/mm^2 and the signal disappears at a b-value of 800 s/mm^2. On the ADC map, the adenoma is isointense and the FNH (arrow) is mildly hyperintense relative to the surrounding liver parenchyma. On the basis of the DWIs the adenoma was classified as indeterminate (a score of 2) and the FNH was correctly judged as benign (a score of 1) by the two readers. On hepatobiliary phase MR images with Gd-EOB-DTPA, the adenoma (asterisk) is characteristically hypointense (which may be explained by the absence of biliary tree development within this tumor) and the FNH (arrow) is mildly hyperintense relative to the surrounding liver parenchyma.

The four benign lesions misjudged as malignant by both readers at DWI included two (3.92%, 2/51) hemangiomas, one (5.88%, 1/17) adenoma, and one (100%, 1/1) abscess.

The five malignant lesions misjudged as benign by both readers at DWI included four lymphomas (80%, 4/5) and one complete necrotic metastasis (2.94%, 1/34). The four lymphomas and one metastasis appeared hyperintense to surrounding liver parenchyma on the ADC map due to uncommonly high ADCs ($\geq 1.12 \times 10^{-3}$mm^2/s). The four HCCs (7.27%, 4/55) were miscategorized as benign at DWI by reader 1. Meanwhile, all false-negative cases of malignant lesions were judged as indeterminate and there were no cases of them misjudged as benign at T2WI.

DISCUSSION

Unenhanced MR sequences are essential in the characterization of FLLs, even in an MR liver protocol that already included a dynamic contrast-enhanced sequence. Both T2WI and DWI play major roles for

that purpose in a clinical setting (9–11,19). Although the roles of T2WI and DWI may be similar in the characterization of FLLs, there are limited data on the comparison between T2WI and DWI, and most previous studies mainly included cysts and hemangiomas as benign lesions (11,19). Advantages and disadvantages of each sequence in the characterization of FLLs have not been fully investigated yet.

Our study showed that the combination of T2WI and DWI could provide significantly higher accuracy in discriminating benign from malignant FLLs than T2WI alone and DWI alone.

In agreement with previous reports (11,19), we also found that almost all cystic benign lesions were correctly characterized with both T2WI and DWI, without any significant differences between the two sequences. Among cystic benign lesions, one hemangioma at T2WI and two hemangiomas at DWI were mischaracterized as malignant lesions. Theses lesions showed decreased signal on T2WI and the ADC map, suggesting a hyalinized hemangioma. As previously reported (32), hyalinized hemangioma changes its radiologic features due to extensive fibrous tissue within the tumor and obliteration of their vascular channels, and it sometimes may be misdiagnosed as malignant tumor. Thus, it should be mentioned that hyalinized hemangioma could show only slight high intensity on T2WI and decreasing its ADC value appearing isointense or slightly hypointense on ADC map. Regarding the discrimination between solid benign and malignant lesions, we found that the diagnostic performance of DWI in the differentiation between solid benign tumors (adenoma and FNH) from malignant FLLs to be better than that of T2WI, although its utility was still limited in adenoma cases (Fig. 3). Particularly in FNH cases, the diagnostic ability with DWI was superior to that with T2WI. Eight FNHs (14.8%, 8/54) were mischaracterized as malignant lesion on T2WI, while no case was observed like this on DWI. The exact reason why the DWI indicated better latent ability for the differentiation is unclear, despite the solid benign tumors showing higher cellularity. We speculate that hypervascularization of solid benign tumors could alter diffusion, as some HCCs also show a false increase in ADC values (33). Moreover, compared to malignant lesions, cellular density of benign solid tumors may basically be lower because the growth speed of malignant tumors is rapid and they grow continuously, while that of benign solid tumors is slower and usually their sizes remain almost unchanged. Additionally, in FNH cases, the presence of a central vascular scar may also be another reason for the better results of the differentiation. Among 19 FNHs, which were identified by a central vascular scar within the tumors on DWI with each b-value and ADC maps, seven (36.8%) were correctly judged as benign using this additional information, although this additional value may be limited for the diagnosis of small FNH (particular less than 3 cm), in which the central scar is possibly absent.

Basically, all image sequences were more accurate in the characterization of malignant FLLs than of benign FLLs ($P < 0.001$). In particular, the accuracies were almost complete for the diagnosis of metastasis and CCC. These malignant tumors usually show typical malignant features, although metastasis with large cystic necrosis, which could show increasing signal and ADC value, may appear as benign tumors, as previous researchers mentioned (34). Meanwhile, the accuracy with DWI for the diagnosis of HCC was inferior to that with T2WI. The four HCCs (7.27%, 4/55) were miscategorized as benign at DWI by reader 1, while all false-negative cases of malignant lesions were judged as indeterminate and there were no cases of them misjudged as benign at T2WI. As some investigators indicated (35,36), the histological grade of HCCs could affect signal intensity of the tumors because DWI is more closely related to the histological changes of hepatocellular lesions than T2WI. More than 90% of moderately or poorly differentiated HCCs appear hyperintense; however, 67% of well-differentiated HCCs appear isointense on DWI (36). Moreover, histological changes of background liver parenchyma, such as fibrosis, fibrous septa, or regenerative nodules could also change the lesion-to-liver contrast on DWI. In some cases that may lead to difficulties of interpretation on ADC maps because of heterogeneity of background liver parenchyma. These factors seem to be attributed to the loss of diagnostic confidence with DWI compared to T2WI in HCC cases. All four lymphoma were misdiagnosed as benign on DWI due to having unusually higher ADC values, although they were correctly judged as malignant on T2WI.

Because of these complementary effects of T2WI and DWI, our study indicates that combined interpretation of them could provide significantly higher accuracy in discriminating benign from malignant FLLs than each single reading of T2WI and DWI. Therefore, these sequences are essential together in the scanning protocols of clinical practice and combined reading could provide better ability in the characterization of FLLs.

This study has several limitations. First, the study design was retrospective and we included patients who had undergone MRI for diagnostic purposes, as part of routine clinical care. Although this may have introduced some bias, we believe that our results are valid because we included a consecutive series of patient during a relatively long period. Second, not all FLLs could be diagnosed histopathologically. Nevertheless, careful consensus reading by experienced abdominal radiologists and follow-up examinations were used to establish a final diagnosis in these cases. Third, in this study we evaluated diagnostic ability with only visual assessment of each image sequence and did not include it in ADC measurements, although we also measured ADC values of all FLLs because the point at issue was more focused. Fourth, DWI and T2WI were not compared to contrast-enhanced MRI in this study. Basically, contrast-enhanced MRI is superior to unenhanced MRI in the characterization of FLLs. However, unenhanced MRI such as T2WI and DWI could provide additional important information, which may not be obtained with contrast-enhanced MRI. Moreover, in those patients with contraindications to contrast agents (eg, patients having contrast agent allergy or impaired

renal function), these sequences become crucial role in the characterization of FLLs.

In conclusion, the characterization accuracy was significantly higher in combined characterization by T2WI and DWI as compared to either of these two imaging modalities alone in all lesions and subgroups of benign and malignant lesions. Regarding a comparison between T2WI and DWI, the characterization accuracy was significantly higher in DWI in the benign lesions but was significantly higher in T2WI in the malignant lesions.

REFERENCES

1. Namimoto T, Yamashita Y, Sumi S, Tang Y, Takahashi M. Focal liver masses: characterization with diffusion-weighted echo-planar MR imaging. Radiology 1997;204:739–744.
2. Ichikawa T, Haradome H, Hachiya J, Nitatori T, Araki T. Diffusion weighted MR imaging with a single-shot echoplanar sequence: detection and characterization of focal hepatic lesions. Am J Roentgenol 1998;170:397–402.
3. Yamada I, Aung W, Himeno Y, Nakagawa T, Shibuya H. Diffusion coefficients in abdominal organs and hepatic lesions: evaluation with intravoxel incoherent motion echo-planar MR imaging. Radiology 1999;210:617–623.
4. Kim T, Murakami T, Takahashi S, Hori M, Tsuda K, Nakamura H. Diffusion-weighted single-shot echoplanar MR imaging for liver disease. Am J Roentgenol 1999;173:393–398.
5. Taouli B, Vilgrain V, Dumont E, Daire JL, Fan B, Menu Y. Evaluation of liver diffusion isotropy and characterization of focal hepatic lesions with two single-shot echo-planar MR imaging sequences: prospective study in 66 patients. Radiology 2003;226:71–78.
6. Yoshikawa T, Kawamitsu H, Mitchell DG, et al. ADC measurement of abdominal organs and lesions using parallel imaging technique. Am J Roentgenol 2006;187:1521–1530.
7. Coenegrachts K, Delanote J, Ter Beek L, et al. Improved focal liver lesion detection: comparison of single-shot diffusion-weighted echoplanar and single-shot T2 weighted turbo spin echo techniques. Br J Radiol 2007;80:524–531.
8. Gourtsoyianni S, Papanikolaou N, Yarmenitis S, et al. Respiratory gated diffusion-weighted imaging of the liver: value of apparent diffusion coefficient measurements in the differentiation between most commonly encountered benign and malignant focal liver lesions. Eur Radiol 2008;18:486–492.
9. Bruegel M, Gaa J, Waldt S, et al. Diagnosis of hepatic metastasis: comparison of respiration-triggered diffusion-weighted echo-planar MRI and five T2-weighted turbo spin-echo sequences. Am J Roentgenol 2008;191:1421–1429.
10. Bruegel M, Holzapfel K, Gaa J, et al. Characterization of focal liver lesions by ADC measurements using a respiratory triggered diffusion diffusion-weighted single-shot echo-planar MR imaging technique. Eur Radiol 2008;18:477–485.
11. Parikh T, Drew SJ, Lee VS, et al. Focal liver lesion detection and characterization with diffusion-weighted MR imaging: comparison with standard breath-hold T2-weighted imaging. Radiology 2008; 246:812–822.
12. Zech CJ, Herrmann KA, Dietrich O, Horger W, Reiser MF, Schoenberg SO. Black-blood diffusion-weighted EPI acquisition of the liver with parallel imaging: comparison with a standard T2-weighted sequence for detection of focal liver lesions. Invest Radiol 2008;43: 261–266.
13. Kamel IR, Bluemke DA, Ramsey D, et al. Role of diffusion-weighted imaging in estimating tumor necrosis after chemoembolization of hepatocellular carcinoma. AJR Am J Roentgenol 2003; 181:708–710.
14. Kamel IR, Bluemke DA, Eng J, et al. The role of functional MR imaging in the assessment of tumor response after chemoembolization in patients with hepatocellular carcinoma. J Vasc Interv Radiol 2006;17:505–512.
15. Koh DM, Scurr E, Collins D, et al. Predicting response of colorectal hepatic metastasis: value of pretreatment apparent diffusion coefficients. AJR Am J Roentgenol 2007;188:1001–1008.
16. Cui Y, Zhang XP, Sun YS, Tang L, Shen L. Apparent diffusion coefficient: potential imaging biomarker for prediction and early detection of response to chemotherapy in hepatic metastases. Radiology 2008;248:894–900.
17. Taouli B, Tolia AJ, Losada M, et al. Diffusion-weighted MRI for quantification of liver fibrosis: preliminary experience. Am J Roentgenol 2007;189:799–806.
18. Taouli B, Chouli M, Martin AJ, Qayyum A, Coakley FV, Vilgrain V. Chronic hepatitis: role of diffusion-weighted imaging and diffusion tensor imaging for the diagnosis of liver fibrosis and inflammation. J Magn Reson Imaging 2008;28:89–95.
19. Yang DM, Jahng GH, Kim HC, et al. The detection and discrimination of malignant and benign focal hepatic lesions: T2 weighted vs. diffusion-weighted MRI. Br J Radiol 2011;84:319–326.
20. Bartolozzi C, Cioni D, Donati F, Lencioni R. Focal liver lesions: MR imaging-pathologic correlation. Eur Radiol 2001;11:1374–1388.
21. Horton KM, Bluemke DA, Hruban RH, Soyer P, Fishman EK. CT and MR imaging of benign hepatic and biliary tumors. Radiographics 1999;19:431–451.
22. Zech CJ, Grazioli L, Breuer J, Reiser MF, Schoenberg SO. Diagnostic performance and description of morphological features of focal nodular hyperplasia in Gd-EOB-DTPA-enhanced liver magnetic resonance imaging: results of a multicenter trial. Invest Radiol 2008;43:504–511.
23. Grazioli L, Bondioni MP, Faccioli N, et al. Solid focal liver lesions: dynamic and late enhancement patterns with the dual phase contrast agent gadobenate dimeglumine. Gastrointest Cancer 2010;41:221–232.
24. Silva AC, Evans JM, McCullough AE, Jatoi MA, Vargas HE, Hara AK. MR imaging of hypervascular liver masses: a review of current techniques. Radiographics 2009;29:385–402.
25. Rimola J, Forner A, Reig M, et al. Cholangiocarcinoma in cirrhosis: absence of contrast washout in delayed phases by magnetic resonance imaging avoids misdiagnosis of hepatocellular carcinoma. Hepatology 2009;50:791–798.
26. Soyer P, Bluemke DA, Reichle R, et al. Imaging of intrahepatic cholangiocarcinoma. 1. Peripheral cholangiocarcinoma. Am J Roentgenol 1995;165:1427–1431.
27. Danet IM, Semelka RC, Leonardou P, et al. Spectrum of MRI appearances of untreated metastases. Am J Roentgenol 2003;181: 809–817.
28. Bruix J, Sherman M. Practical Guidelines Committee, American Association for the Study of Liver Disease. Management of hepatocellular carcinoma. Hepatology 2005;42:1208–1236.
29. Lombardo DM, Baker ME, Spritzer CE, Blinder R, Meyers W, Herfkens RJ. Hepatic hemangiomas vs metastases: MR differentiation at 1.5 T. AJR Am J Roentgenol 1990;155:55–59.
30. Shinmura R, Matsui O, Kobayashi S, et al. Cirrhotic nodules: association between MR imaging signal intensity and intranodular blood supply. Radiology 2005;237:512–519.
31. Farraher SW, Jara H, Chang KJ, Ozonoff A, Soto JA. Differentiation of hepatocellular carcinoma and hepatic metastasis from cysts and hemangiomas with calculated T2 relaxation times and the T1/T2 relaxation times ratio. J Magn Reson Imaging 2006; 24:1333–1341.
32. Cheng HC, Tsai SH, Chiang JH, Chang CY. Hyalinized liver hemangioma mimicking malignant tumor at MR imaging (Letter). Am J Roentgenol 1995;165:1016–1017.
33. Xu H, Li X, Xie JX, et al. Diffusion-weighted magnetic resonance imaging of focal hepatic nodules in an experimental hepatocellular carcinoma rat model. Acad Radiol 2007;14:279–286.
34. Chan JH, Tsui EY, Luk SH. Diffusion-weighted MR imaging of the liver: distinguishing hepatic abscess from cystic or necrotic tumor. Abdom Imaging 2001;26:161–165.
35. Nasu K, Kuroki Y, Tsukamoto T, et al. Diffusion-weighted imaging of surgically resected hepatocellular carcinoma: imaging characteristics and relationship among signal intensity, apparent diffusion coefficient, and histopathologic grade. Am J Roentgenol 2009;193:438–444.
36. Muhi A, Ichikawa T, Motosugi U, et al. High-b-value diffusion-weighted MR imaging of hepatocellular lesions: estimation of grade of malignancy of hepatocellular carcinoma. J Magn Reson Imaging 2009;30:1005–1011.